

Accepted Manuscript

Title: High capacity cryogel-type adsorbents for protein purification

Author: Naveen Kumar Singh Roy N. Dsouza Mariano
Grasselli Marcelo Fernández-Lahore



PII: S0021-9673(14)00889-9
DOI: <http://dx.doi.org/doi:10.1016/j.chroma.2014.06.008>
Reference: CHROMA 355484

To appear in: *Journal of Chromatography A*

Received date: 5-3-2014
Revised date: 2-6-2014
Accepted date: 3-6-2014

Please cite this article as: N.K. Singh, R.N. Dsouza, M. Grasselli, M. Fernández-Lahore, High capacity cryogel-type adsorbents for protein purification, *Journal of Chromatography A* (2014), <http://dx.doi.org/10.1016/j.chroma.2014.06.008>

This is a PDF file of an unedited manuscript that has been accepted for publication. As a service to our customers we are providing this early version of the manuscript. The manuscript will undergo copyediting, typesetting, and review of the resulting proof before it is published in its final form. Please note that during the production process errors may be discovered which could affect the content, and all legal disclaimers that apply to the journal pertain.

1 **High capacity cryogel-type adsorbents for protein purification**

2

3 Naveen Kumar Singh¹, Roy N. Dsouza¹, Mariano Grasselli² and Marcelo Fernández-
4 Lahore^{1*}

5

6

7 ¹*Downstream Bioprocessing Laboratory, School of Engineering and Science, Jacobs*
8 *University, Campus Ring 1, D-28759 Bremen, Germany*

9 ²*Laboratorio de Materiales Biotecnológicos, Depto. de Ciencia y Tecnología, Universidad*
10 *Nacional de Quilmes, Roque Sáenz Peña 352 (B1876BXD) Bernal, Argentina*

11

12

13

14 *Correspondence to:

15 Prof. Dr. Marcelo Fernández-Lahore,
16 Downstream BioProcessing Laboratory,
17 Jacobs University, Campus Ring 1,
18 D-28759 Bremen, Germany.

19 Phone: +49 421 200 3239,

20 Fax: +49 421 200 3600.

21 E-mail: m.fernandez-lahore@jacobs-university.de

22

23

23 **ABSTRACT**

24 Cryogel bodies were modified to obtain epoxy groups by graft-copolymerization
25 using both chemical and gamma irradiation initiation techniques. The free epoxy adsorbents
26 were reacted further to introduce diethylaminoethanol (DEAE) functionalities. The resulting
27 weak anion-exchange cryogel adsorbents showed dynamic binding capacities of *ca.* 27 ± 3
28 mg/mL, which was significantly higher than previously reported for this type of adsorbent
29 material. Gamma irradiated grafting initiation showed a 4-fold higher capacity for proteins
30 than chemical grafting initiation procedures. The phosphate capacity for these DEAE
31 cryogels was 119 mmol/L and also showed similar column efficiency as compared to
32 commercial adsorbents. The large pores in the cryogel structure ensure convective transport
33 of the molecules to active binding sites located on the polymer-grafted surface of cryogels.
34 However, as cryogels have relatively large pores (10 - 100 μm), the BET area available for
35 surface activation is low, and consequently, the capacity of the cryogels is relatively low for
36 biomolecules, especially when compared to commercial beaded adsorbents. Nevertheless, we
37 have shown that gamma ray mediated surface grafting of cryogel matrices greatly enhance
38 their functional and adsorptive properties..

39

40 **Keywords:** megaporous cryogels; protein chromatography; weak anion-exchange; dynamic
41 binding capacity; monoliths.

42

43

44

45

46

47

48

49

50

50 1. Introduction

51 Recent advancement in genetic engineering and recombinant DNA technology has
52 boosted the demand for the recombinant and natural proteins as well as for large
53 biomolecules like plasmid DNA and virus-like particles. The biggest concern for the
54 biopharmaceutical industry is to deliver these new therapeutic products to a highly
55 demanding and regulated market [1] While upstream production of such biomolecules has
56 made significant strides in terms of product yield, the major bottleneck lies in their
57 downstream bioprocessing and purification, which needs to be simplified and made cost-
58 effective [2-4]. Anion-exchange chromatography is one such purification methodology,
59 which is widely used for isolating proteins under neutral or slightly basic pH conditions [5-7].
60 Commonly used weak anion-exchangers contain diethylaminoethyl (DEAE) or
61 polyethyleneimine (PEI) functionalities, whereas quaternary (Q) amines are used as strong
62 anion-exchangers [8, 9].

63 As a result of their simple preparation and enhanced mass transfer properties,
64 monolithic cryogels present an attractive alternative to currently used beaded adsorbent
65 media. In this paper, we have prepared monolithic cryogels which offer several advantages
66 over other commercial adsorbents. The structural aspects of these adsorbents allow the
67 separation and purification of biomolecules that is independent of flow rate and while
68 maintaining efficient mass transfer as compared to the limited operating pressures required
69 by conventional particle based resins. In earlier studies, cryogel-based weak anion-
70 exchangers (WAX) were prepared by appending DEAE groups onto their epoxy-
71 functionalized backbone [8]. Such functionalities have been introduced either directly during
72 the preparation of the cryogel backbone [9-11] or by surface grafting, where the epoxy
73 groups are first introduced onto the cryogel and subsequently modified into any desired
74 functionality [8]. For example, Gu *et al.* adopted the former approach and synthesized a
75 series of monoliths using functionalized copolymers with strong cation-exchange properties
76 in a single step [8, 12, 13]. On the other hand, various materials have also been synthesized
77 by adding ionizable groups onto the backbone of monoliths by surface grafting For example,
78 anion-exchangers like poly[2-(dimethylamino)ethyl methacrylate] (pDMAEMA) and poly[2-
79 methacryloxy)ethyl trimethylammonium chloride] (pMETAC) were chemically grafted with
80 functional polymers using potassium diperiodatocuprate as radical initiator, and reported
81 protein-binding capacities of up to 6-12 mg/mL [14].

82 Various kind of radical initiation techniques, i.e., chemical [11], photo-initiation [15]
83 and gamma irradiation [16], have been employed to graft-polymerize acrylate-based
84 derivatives for adding epoxide groups onto monolithic adsorbents. In the present study, GMA
85 was graft-polymerized onto monolithic cryogels using both chemical as well as gamma
86 irradiation initiation techniques. Compared to previous reports [16, 17], the scope of this
87 work is to compare the effects of using different graft-initiation procedures to develop
88 efficient weak anion-exchange adsorbents. Their physico-chemical properties were
89 characterized by various methods, while their chromatographic properties were assessed in
90 terms of the binding capacities of BSA at various operational flows rates.

91 **2. Material and methods**

92 **2.1. Chemicals and reagents**

93 Methacrylic acid (MAA), ethylene glycol dimethacrylate (EGDMA), polyethylene
94 glycol dimethacrylate (PEGDA), glycidyl methacrylate (GMA), diethylamine (DEA 99.5%),
95 dimethylamine (40%), ammonium cerium (IV) nitrate (CAN), N,N-dimethylacrylamide
96 (DMA), and bovine serum albumin (BSA) were purchased from Sigma-Aldrich (Germany).
97 Acetone, ammonium persulfate (APS), sodium dihydrogen phosphate, disodium hydrogen
98 phosphate, sodium chloride (NaCl), N,N,N',N'-Tetramethylethylenediamine (TEMED),
99 sodium hydroxide (NaOH), nitric acid (HNO₃, 65%) were purchased from AppliChem
100 (Germany). Tris (99.3%, buffer grade) was purchased from Carl Roth (Germany). Ethanol
101 absolute was purchased from Honeywell specialty chemicals Seelze GmbH (Seelze,
102 Germany).

103 Buffer solutions were filtered through a 0.45 µm cellulose acetate filter (Sartorius,
104 Goettingen, Germany).

105 **2.2. Instrumentation**

106 Tricorn chromatography columns 10/50 (10 mm internal diameter (i.d.) × 4 cm
107 length) and the ÄKTA explorer 100, controlled by Unicorn 4.10 software, were obtained
108 from GE Amersham Bioscience (Uppsala, Sweden). Absorbance was measured at 280 nm
109 for the static capacity determination and was performed using a Shimadzu UV-1700
110 PharmaSpec spectrophotometer.

111 Dehydrated monolithic cryogels were coated with gold, and the samples were
112 examined at different magnification using a Joel JSM 5900 (Peabody Inc., USA) scanning

113 electron microscope (SEM).

114 **2.3. Cryogel synthesis and characterization**

115 **2.3.1. Preparation of the cryogel backbone**

116 Megaporous cryogels were prepared as follows: the monomer, MAA (230 mmol), the
117 cross-linkers, PEGDA (95 mmol) and EGDMA (32 mmol), and the catalyst, TEMED (80
118 mmol), were dissolved in water to give a final volume of 30 mL. This solution was degassed
119 with nitrogen for 20 minutes. Subsequently, APS (27 mmol) was added as an initiator as
120 described previously [16]. The final solution was poured in plastic syringes (16 mm inner
121 diameter, 7 cm height) and kept at $-20\text{ }^{\circ}\text{C}$ for 24 hours. The resulting cryogels were thawed
122 at room temperature, washed with 200 mL water, and dried at $60\text{ }^{\circ}\text{C}$ overnight.

123 **2.3.2. Chemical grafting (CG) procedure**

124 A 0.4 g of dried adsorbents was first grafted with 2.5 ml GMA and 50 mg CAN as an
125 initiator containing 31.25 mL of nitrogen purged water (0.1 M nitric acid) for 3 hours at 40
126 $^{\circ}\text{C}$. The grafted monolithic cryogels was extensively washed with tap water until a neutral pH
127 was achieved and then dried at $50\text{ }^{\circ}\text{C}$ as described previously [17].

128 **2.3.3. Gamma irradiation (GIR) grafting procedure**

129 A known amount of dried adsorbent was soaked in 50 mL of a nitrogen-purged (20
130 minutes) monomer solution of GMA (3.2% v/v) and DMA (7.6% v/v) in ethanol/water (1:1
131 v/v). The mixture was enclosed in a sealed tube to avoid oxygen diffusion during irradiation,
132 which may hamper the grafting. Samples were irradiated with a 10 kGy dose at room
133 temperature (Beta Gamma Service GmbH and Co. KG, Wiehl, Germany). After irradiation,
134 the resulting material was first washed with ethanol/water (1:1 v/v) followed with 96%
135 ethanol and subsequently dried at $50\text{ }^{\circ}\text{C}$ in a vacuum oven [16, 18].

136 **2.3.4. Surface functionalization by DEAE groups**

137 The epoxy groups present on the monolithic cryogels were modified into DEAE
138 groups by reacting them with an aqueous solution of diethylamine (25% v/v), dimethylamine
139 (25% v/v), and ethanol (10% v/v). Finally, the functionalized monolithic cryogels were
140 extensively washed with deionized water until a neutral pH was obtained, and subsequently
141 dried at $50\text{ }^{\circ}\text{C}$ in a vacuum oven [19].

142 2.3.5. Physico-chemical characterization

143 The functionalized cryogels were characterized in numerous ways, including SEM
144 (see Figure 2). The degree of grafting (DG) was measured by the elementary weight gain
145 before (W_0) and after (W_1) grafting [17] as shown in Equation 1.

$$146 \quad DG \text{ (g/g)} = \frac{(W_1 - W_0)}{W_0} \times 100 \quad (1)$$

147 Additionally, the degree of swelling (DS) was measured by weighing the monolithic
148 cryogels in the wet state (m_{wet}) and dried state (m_{dry}) until constant weight was achieved at
149 60 °C in a vacuum oven [18]. DS was calculated using Equation 2.

$$150 \quad DS \text{ (g/g)} = \frac{(m_{wet} - m_{dry})}{m_{dry}} \quad (2)$$

151 Finally, the porosity of the monolithic cryogels was estimated by water uptake
152 (Equation 3). A cryogel sample, 3.5 cm in length, was saturated with deionized water. The
153 mass of the wet material saturated with deionized water was denoted as $m_{swollen}$ and the
154 material was squeezed to remove the excess free water present within the large pores as
155 previously reported [18], and the mass of squeezed material was denoted as $m_{squeezed}$. The
156 porosity of the “squeezed” swollen sample was calculated using Equation 3.

$$157 \quad \text{Porosity (\%)} = \frac{[m_{swollen} - m_{squeezed}]}{m_{swollen}} \times 100 \quad (3)$$

158 2.4 Column efficiency & ionic capacity

159 The monolithic cryogels were packed into Tricorn 10/50 columns and swollen in
160 place with 20 mM Tris-HCl buffer (pH 7.4) at very low linear flow velocity (~ 75 cm/h). The
161 column bed height was fixed so that there was no visible headspace in the column. The
162 efficiency of the packed column was evaluated in terms of HETP by using 5% acetone (v/v)
163 at flow velocities ranging from 75 to 600 cm/h.

164 A measure of ion-exchange capacity of adsorbents can be determined using transient
165 pH measurements from which the number of phosphate ions binding to the adsorbent can be
166 calculated [20]. These “phosphate capacities” were evaluated by using two buffer solutions
167 having same pH, but with different ionic strengths. The functionalized cryogels were
168 equilibrated with 500 mM phosphate buffer at pH 7.4. The mobile phase composition was

169 then switched to 20 mM phosphate buffer at the same pH. The change in ion concentration
 170 induces a change in observed pH as a result of the release of ions that were bound to the
 171 matrix in high salt conditions. The time interval of this change, Δt ($|\Delta \text{pH}| > 0$), was
 172 determined by monitoring the time required in between the switching point of the mobile
 173 phase and the point at which 50% of the maximum change in pH value is attained (see
 174 Figure 3). The “phosphate capacity” (K) depends upon the volumetric flow rate (ϕ_v), the
 175 column volume (V_c), the concentration of elution buffer (C_2), as well as Δt [18, 21, 22], as
 176 shown in Equation 4..

$$177 \quad K = \frac{[\Delta t(\text{pH})_{50\%} \times \phi_v]}{V_c} \quad (4)$$

178 2.5. Static and Dynamic Binding Capacities

179 Static binding capacity (SBC) of the weak anion-exchange adsorbents was determined by
 180 batch adsorption experiments with BSA. Cryogels were equilibrated with 20 mM phosphate
 181 buffer (pH 7.4) and were subsequently incubated with 10 mg/mL of BSA at room
 182 temperature for 3 h. The amount of BSA adsorbed was determined by the differences in the
 183 absorbance (OD_{280}) of BSA before and after incubation. Controls experiments revealed
 184 negligible non-specific binding of BSA to the non-functionalized adsorbent.

185 The dynamic binding capacity (DBC) at 10% breakthrough for the BSA with CG- or
 186 GIR-DEAE cryogels was determined by frontal studies [23]. The Tricorn 10/50 column was
 187 packed and mounted to an ÄKTA explorer 100 system and equilibrated with 20 mM Tris-
 188 HCl buffer at pH 7.4. A solution of BSA (2 mg/mL) was loaded at linear flow velocities
 189 ranging from 75 - 600 cm/h. The breakthrough volume (V) of the protein solution that was
 190 needed to saturate the column was determined by monitoring the UV absorbance at 280 nm
 191 [24]. The bound protein was eluted with 1 M NaCl in 20 mM Tris-HCl buffer. The dynamic
 192 binding capacities of the adsorbents can be calculated from the initial load concentration
 193 (C_0), breakthrough volume (V), column void volume (V_0), as well as either the dry weight of
 194 the adsorbent (W_g) or its volume (CV), as shown in Equations 5 and 6 [17].

$$195 \quad \text{DBC (mg/g)} = \frac{C_0 \times (V - V_0)}{W_g} \quad (5)$$

$$196 \quad \text{DBC (mg/mL)} = \frac{C_0 \times (V - V_0)}{CV} \quad (6)$$

197 3. Results and discussion

198 The cryogel backbone forms at $-20\text{ }^{\circ}\text{C}$ by proper mixing of monomers (MAA) and
199 cross-linkers (PEGDA and EGDMA). During the preparation of the backbone, the water that
200 was used as a solvent simultaneously acts as a porogen in the form of ice crystals that are
201 created during the freezing process. This results in pore sizes ranging from $10 - 100\text{ }\mu\text{m}$ [16,
202 25]. Additionally, the crosslinkers, like PEGDA and EGDMA, provide an excellent
203 mechanical stability to the final backbone of cryogels. They were activated with epoxy
204 groups either by chemical or by gamma irradiation initiation techniques (see Figure 1), where
205 the purpose of using GMA as a graft monomer was two-fold. Firstly, chain elongation in the
206 absence of cross-linkers leads to the formation of a thin film of flexible polymeric tentacles
207 which in turn minimizes unfavorable steric effects that may hinder consequent
208 functionalization as well as product adsorption [26, 27]. Secondly, the epoxide group can be
209 further transformed to impart a range of different functionalities to the material, for example,
210 anion-exchange [27-29], cation-exchange [6, 26, 30], or metal-ion chelating capabilities [17,
211 31]. The efficiency of grafting depends upon several parameters like monomer concentration,
212 initiator concentration, reaction time as well as temperature, which were optimized for this
213 study.

214 Water uptake experiments revealed adsorbent porosities of $ca. 70 \pm 5\%$, which
215 indicates that both grafting procedures did not affect the physical integrity of the pores
216 present within the material. The water content in these sponge-like materials could be easily
217 removed by squeezing. They rapidly regain their original size and shape when re-immersed
218 in water, thereby showing remarkable elasticity [16, 25]. Their degree of swelling was $2.4 \pm$

219 0.2 g/g in distilled water at $24\text{ }^{\circ}\text{C}$, and indicated their remarkably good convective flow

220 properties. The porous structure of these cryogels was further investigated by SEM, as shown
221 in Figure 2. These images suggest that the pores within the cryogels in their dehydrated state
222 are inter-connected and that their pore sizes range from $10 - 100\text{ }\mu\text{m}$ [16, 25] with an average
223 pores size estimated at $50\text{ }\mu\text{m}$, which is maintained in the hydrated as well (see Supporting
224 Information).

225 In the same manner as reported by Plieva et al. [32, 33], the cryogel matrices have

226 been synthesized within the syringes and ‘re-packed’ into chromatography columns by
227 placing the entire cryogel directly into these columns in their dehydrated state. The sponge-
228 like characteristics of polymethacrylate-based cryogels upon swelling ensure uniform and
229 sufficiently tight ‘packing’ into the column. The advantage of this process over in-column
230 monoliths is in the ease of further functionalization of the matrices, which is necessary for
231 surface grafting. The column efficiency of chromatographic adsorbents are vital for their
232 application in purification systems. The theoretical plate height (HETP) is one such property
233 that determines the overall separation efficiency of a chromatographic column. Using acetone
234 as a non-interacting probe solute, the HETP of the cryogel column was measured (see Figure
235 3), and the relation between HETP and flow velocity for CG-DEAE and GIR-DEAE was
236 established. In general, desirable HETPs for these materials result from plate heights ranging
237 from 0.5 - 1 mm. In the case of CG-DEAE, these plate heights were unfortunately not
238 realized irrespective of flow rate. However, the plate heights for GIR-DEAE cryogels fell
239 within the sought out range (0.53 - 0.73 mm), thereby highlighting the distinct advantage of
240 the grafted cryogels generated from gamma irradiation as compared to chemical initiation.
241 We therefore decided to focus further adsorption experiments on GIR-DEAE cryogels

242 The phosphate capacity for GIR-DEAE monolithic cryogels measured by the pH
243 transient method was 119 mmol/L (see Figure 4) [34], and was comparable to the
244 commercially available DEAE sepharose fast flow adsorbents obtained at similar conditions
245 to be 113 mmol/L (0.11-0.16 mmol/mL chloride ion capacity reported by GE Healthcare).
246 Subsequently, more detailed mass transfer studies on the protein binding capacities of the
247 cryogels, in static as well as dynamic modes, were conducted by using BSA a model protein.
248 The effect of different grafting initiator was determined by frontal analysis (see Table 1 and
249 Figure 5), where it was clear that the highest dynamic binding capacity (DBC) was obtained
250 at 75% degree of grafting with a value of 110 ± 10 mg/g. The corresponding static binding
251 capacity, obtained with 10 mg/mL BSA solution, was 180 ± 20 mg/g.

252 Generally, the degree of grafting is directly correlated with the number of ionic sites
253 on the matrix, and consequently, the binding capacity for the protein. Counterintuitively,
254 however, breakthrough studies revealed that even though the degree of chemically initiated
255 grafting (93%) was higher compared to that for gamma irradiation (75%), its binding
256 capacity for BSA was *ca.* 3 - 4 fold lower (see Figure 5). The results of the breakthrough
257 experiments carried out at different flow rates (at high flow rate) for the adsorbents are
258 expressed by the DBC were compared and contrasted with other reported adsorbents as

259 shown in Table 1. A clear existence of mass transfer resistance with increasing flow rates is
260 observed. The 10% DBC values for CG-DEAE and GIR-DEAE were measured as 5 ± 2
261 mg/mL and 27 ± 3 mg/mL, respectively, and these values are higher or comparable to the
262 DBC values reported in the literature for various monoliths, for example, weak anion-
263 exchange (WAX) pAAm cryogels [27], BIA Separations monolith adsorbents (CIM DEAE
264 disks) [11], and PEI modified WAX on a poly(GMA-co-EDMA) [35]. Furthermore, at higher
265 flow rates, GIR-DEAE showed higher binding capacities for BSA than selected traditional
266 commercial beads available in the market (Toyopearl DEAE 650M, MacroPrep DEAE) [36].
267 DBCs of 42 mg/mL were obtained from our experiments with DEAE Sepharose FF at a flow
268 rate of 300 cm/h. However, DEAE sepharose Fast Flow and DEAE Ceramic Hyper D 20
269 outperformed the WAX cryogel synthesized in the current report [36]. The lower DBC values
270 compared to particulate chromatographic media are due to lower accessible surface area in
271 cryogels, where it is evident from the SEM images that the monolithic cryogels have pore
272 sizes in the range of 10-100 μm (see Figure 2).

273 It has been reported in the literature that the particulate chromatographic media has
274 about 2 - 3 times the surface area of highly porous monoliths [37]. The accessible surface
275 area of cryogels, however, may possibly be increased either by reducing the pore sizes during
276 backbone formation or by increasing the length of polymer chains for introduction of epoxy
277 groups. Nevertheless, the dynamic binding capacities of our cryogels for BSA were
278 independent of flow rates of up to 600 cm/h, ensuring convective flow distribution. This was
279 evident from the negligible reduction in binding capacity they displayed (27 ± 3 mg/mL for
280 GIR-DEAE) when compared to commercial available packed bed adsorbents, where DBCs
281 are reduced by almost half upon increase in flow rates. Additionally, the Péclet number for
282 GIR-DEAE decreases with an increase in flow rate suggesting negligible axial mixing (see
283 Figure 5), and the obtained Péclet numbers of 77 and above additionally confirm the
284 favorable plug flow characteristics of these cryogels. The cryogel matrices are scalable by
285 connecting the matrices in series within a column to any production scale without losing its
286 efficiency [38-41].

287 **4. Conclusions**

288 We have illustrated two different ways to efficiently graft GMA onto monolithic
289 cryogels. In the case of gamma irradiation graft-initiation, about 75% grafting was possible.
290 The results of this study also demonstrated that gamma irradiated DEAE monolithic cryogels
291 exhibit a 4-fold higher binding capacity for BSA than their chemically grafted counterparts.

292 The highest binding capacity of 110 ± 10 mg/g was achievable at 75% degree of grafting. It
293 might even be possible to further increase this capacity by reducing the pore sizes of the
294 cryogels. Since the hydrodynamic properties were preserved, grafted cryogels may become a
295 resin of choice for the downstream processing of various biomolecules. Furthermore, these
296 adsorbent matrices were shown to have relatively higher capacities for protein at high flow
297 rates. Not only are these cryogels considerably cheaper than commercially available
298 adsorbents, they have also be shown to be easily scalable [42].

299

300 **Acknowledgements**

301 The authors thank Mirna Sanchez for helping out with sample preparation for gamma
302 irradiation. M.F.L. and M.G. are members of the National Council for Science and
303 Technology, Buenos Aires, Argentina. This work is funded by the European Union Seventh
304 Framework Programme (FP7/2007-2013) under grant agreement n°312004.

305 **References:**

- 306 [1] H.L. Knudsen, R.L. Fahrner, Y. Xu, L.A. Norling, G.S. Blank, Membrane ion-exchange
307 chromatography for process-scale antibody purification, *J. Chromatogr. A* 907 (2001) 145-
308 154.
- 309 [2] T.-W. Chiou, S. Murakami, D.I.C. Wang, W.-T. Wu, A fiber-bed bioreactor for
310 anchorage-dependent animal cell cultures: Part I. Bioreactor design and operations,
311 *Biotechnol. Bioeng.* 37 (1991) 755-761.
- 312 [3] E. Hallgren, F. Kálmán, D. Farnan, C. Horváth, J. Ståhlberg, Protein retention in ion-
313 exchange chromatography: effect of net charge and charge distribution, *J. Chromatogr. A* 877
314 (2000) 13-24.
- 315 [4] A.C.A. Roque, C.R. Lowe, M.Â. Taipa, Antibodies and Genetically Engineered Related
316 Molecules: Production and Purification, *Biotechnol. Prog.* 20 (2004) 639-654.
- 317 [5] S.-H. Chang, R. Noel, F.E. Regnier, High speed ion exchange chromatography of
318 proteins, *Anal. Chem.* 48 (1976) 1839-1845.
- 319 [6] S. Gupta, E. Pfannkoch, F.E. Regnier, High-performance cation-exchange
320 chromatography of proteins, *Anal. Biochem.* 128 (1983) 196-201.
- 321 [7] G. Vanecek, F.E. Regnier, Variables in the high-performance anion-exchange
322 chromatography of proteins, *Anal. Biochem.* 109 (1980) 345-353.
- 323 [8] Y. Li, B. Gu, H. Dennis Tolley, M.L. Lee, Preparation of polymeric monoliths by
324 copolymerization of acrylate monomers with amine functionalities for anion-exchange
325 capillary liquid chromatography of proteins, *J. Chromatogr. A* 1216 (2009) 5525-5532.
- 326 [9] W. Wieder, C.P. Bisjak, C.W. Huck, R. Bakry, G.K. Bonn, Monolithic poly(glycidyl
327 methacrylate-co-divinylbenzene) capillary columns functionalized to strong anion exchangers
328 for nucleotide and oligonucleotide separation, *J. Sep. Sci.* 29 (2006) 2478-2484.

- 329 [10] C.P. Bisjak, R. Bakry, C.W. Huck, G.K. Bonn, Amino-Functionalized Monolithic
330 Poly(glycidyl methacrylate-co-divinylbenzene) Ion-Exchange Stationary Phases for the
331 Separation of Oligonucleotides, *Chroma* 62 (2005) s31-s36.
- 332 [11] V. Frankovič, A. Podgornik, N.L. Krajnc, F. Smrekar, P. Krajnc, A. Štrancar,
333 Characterisation of grafted weak anion-exchange methacrylate monoliths, *J. Chromatogr. A*
334 1207 (2008) 84-93.
- 335 [12] B. Gu, Z. Chen, C.D. Thulin, M.L. Lee, Efficient Polymer Monolith for Strong Cation-
336 Exchange Capillary Liquid Chromatography of Peptides, *Anal. Chem.* 78 (2006) 3509-3518.
- 337 [13] B. Gu, Y. Li, M.L. Lee, Polymer Monoliths with Low Hydrophobicity for Strong
338 Cation-Exchange Capillary Liquid Chromatography of Peptides and Proteins, *Anal. Chem.*
339 79 (2007) 5848-5855.
- 340 [14] I.N. Savina, I.Y. Galaev, B. Mattiasson, Ion-exchange macroporous hydrophilic gel
341 monolith with grafted polymer brushes, *J. Mol. Recognit.* 19 (2006) 313-321.
- 342 [15] E.G. Vlahk, T.B. Tennikova, Preparation of methacrylate monoliths, *J. Sep. Sci.* 30
343 (2007) 2801-2813.
- 344 [16] N.S. Bibi, P.R. Gavara, S.L.S. Espinosa, M. Grasselli, M. Fernández-Lahore, Synthesis
345 and performance of 3D-Megaporous structures for enzyme immobilization and protein
346 capture, *Biotechnol. Progr.* 27 (2011) 1329-1338.
- 347 [17] N.S. Bibi, N.K. Singh, R.N. Dsouza, M. Aasim, M. Fernández-Lahore, Synthesis and
348 performance of megaporous immobilized metal-ion affinity cryogels for recombinant protein
349 capture and purification, *J. Chromatogr. A* 1272 (2013) 145-149.
- 350 [18] P.R. Gavara, R. Cabrera, R.R. Vennapusa, M. Grasselli, M. Fernandez-Lahore,
351 Preparation, characterization, and process performance of composite fibrous adsorbents as
352 cation exchangers for high throughput and high capacity bioseparations, *J. Chromatogr. B*
353 903 (2012) 14-22.
- 354 [19] E. Müller, Comparison between mass transfer properties of weak-anion-exchange resins
355 with graft-functionalized polymer layers and traditional ungrafted resins, *J. Chromatogr. A*
356 1006 (2003) 229-240.
- 357 [20] M.R. Schure, R.S. Maier, How does column packing microstructure affect column
358 efficiency in liquid chromatography?, *J. Chromatogr. A* 1126 (2006) 58-69.
- 359 [21] N. Lendero, J. Vidič, P. Brne, V. Frankovič, A. Štrancar, A. Podgornik, Characterization
360 of ion exchange stationary phases via pH transition profiles, *J. Chromatogr. A* 1185 (2008)
361 59-70.
- 362 [22] F.M. Plieva, J. Andersson, I.Y. Galaev, B. Mattiasson, Characterization of
363 polyacrylamide based monolithic columns, *J. Sep. Sci.* 27 (2004) 828-836.
- 364 [23] E. Boschetti, J.L. Coffman, Enhanced Diffusion Chromatography and Related Sorbents
365 for Biopurification, in: *Bioseparation and Bioprocessing*, Wiley-VCH Verlag GmbH, 2008,
366 pp. 157-198.
- 367 [24] Y.-B. Yang, K. Harrison, J. Kindsvater, Characterization of a novel stationary phase
368 derived from a hydrophilic polystyrene-based resin for protein cation-exchange high-
369 performance liquid chromatography, *J. Chromatogr. A* 723 (1996) 1-10.
- 370 [25] P. Arvidsson, F.M. Plieva, V.I. Lozinsky, I.Y. Galaev, B. Mattiasson, Direct
371 chromatographic capture of enzyme from crude homogenate using immobilized metal

- 372 affinity chromatography on a continuous supermacroporous adsorbent, *J. Chromatogr. A* 986
373 (2003) 275-290.
- 374 [26] M. Kim, S. Kiyohara, S. Konishi, S. Tsuneda, K. Saito, T. Sugo, Ring-opening reaction
375 of poly-GMA chain grafted onto a porous membrane, *J. Membr. Sci.* 117 (1996) 33-38.
- 376 [27] I.N. Savina, I.Y. Galaev, B. Mattiasson, Anion-exchange supermacroporous monolithic
377 matrices with grafted polymer brushes of N,N-dimethylaminoethyl-methacrylate, *J.*
378 *Chromatogr. A* 1092 (2005) 199-205.
- 379 [28] I. Koguma, K. Sugita, K. Saito, T. Sugo, Multilayer Binding of Proteins to Polymer
380 Chains Grafted onto Porous Hollow-Fiber Membranes Containing Different Anion-Exchange
381 Groups, *Biotechnol. Prog.* 16 (2000) 456-461.
- 382 [29] A. Nordborg, E. Hilder, Recent advances in polymer monoliths for ion-exchange
383 chromatography, *Anal. Bioanal. Chem.* 394 (2009) 71-84.
- 384 [30] M. Kim, K. Saito, Radiation-induced graft polymerization and sulfonation of glycidyl
385 methacrylate on to porous hollow-fiber membranes with different pore sizes, *Radiat. Phys.*
386 *Chem.* 57 (2000) 167-172.
- 387 [31] G. Güçlü, G. Gürdağ, S. Özgümüş, Competitive removal of heavy metal ions by
388 cellulose graft copolymers, *J. Appl. Polym. Sci.* 90 (2003) 2034-2039.
- 389 [32] F.M. Plieva, M. Karlsson, M.-R. Aguilar, D. Gomez, S. Mikhailovsky, I.Y. Galaev, Pore
390 structure in supermacroporous polyacrylamide based cryogels, *Soft Matter* 1 (2005) 303-309.
- 391 [33] F.M. Plieva, I.N. Savina, S. Deraz, J. Andersson, I.Y. Galaev, B. Mattiasson,
392 Characterization of supermacroporous monolithic polyacrylamide based matrices designed
393 for chromatography of bioparticles, *J. Chromatogr. B* 807 (2004) 129-137.
- 394 [34] N. Lendero, J. Vidič, P. Brne, A. Podgornik, A. Štrancar, Simple method for
395 determining the amount of ion-exchange groups on chromatographic supports, *J.*
396 *Chromatogr. A* 1065 (2005) 29-38.
- 397 [35] M. Wang, J. Xu, X. Zhou, T. Tan, Preparation and characterization of polyethyleneimine
398 modified ion-exchanger based on poly(methacrylate-co-ethylene dimethacrylate) monolith, *J.*
399 *Chromatogr. A* 1147 (2007) 24-29.
- 400 [36] A. Staby, R.H. Jensen, M. Bensch, J. Hubbuch, D.L. Dünweber, J. Krarup, J. Nielsen,
401 M. Lund, S. Kidal, T.B. Hansen, I.H. Jensen, Comparison of chromatographic ion-exchange
402 resins: VI. Weak anion-exchange resins, *J. Chromatogr. A* 1164 (2007) 82-94.
- 403 [37] F.C. Leinweber, U. Tallarek, Chromatographic performance of monolithic and
404 particulate stationary phases: Hydrodynamics and adsorption capacity, *J. Chromatogr. A*
405 1006 (2003) 207-228.
- 406 [38] G.R. Jespersen, A.L. Nielsen, F. Matthiesen, H.S. Andersen, H. Kirsebom, Dual
407 application of cryogel as solid support in peptide synthesis and subsequent protein-capture, *J.*
408 *Appl. Polym. Sci.* 130 (2013) 4383-4391.
- 409 [39] V.I. Lozinsky, I.Y. Galaev, F.M. Plieva, I.N. Savina, H. Jungvid, B. Mattiasson,
410 Polymeric cryogels as promising materials of biotechnological interest, *Trends Biotechnol.*
411 21 (2003) 445-451.
- 412 [40] F.M. Plieva, I.Y. Galaev, B. Mattiasson, Macroporous gels prepared at subzero
413 temperatures as novel materials for chromatography of particulate-containing fluids and cell
414 culture applications, *J. Sep. Sci.* 30 (2007) 1657-1671.

415 [41] F.M. Plieva, E.D. Seta, I.Y. Galaev, B. Mattiasson, Macroporous elastic polyacrylamide
416 monolith columns: processing under compression and scale-up, *Sep. Purif. Technol.* 65
417 (2009) 110-116.

418 [42] A. Podgornik, M. Barut, A. Štrancar, D. Josić, T. Koloini, Construction of Large-
419 Volume Monolithic Columns, *Anal. Chem.* 72 (2000) 5693-5699.

420

421

Accepted Manuscript

421

422 **Figure Captions**

423 **Figure 1:** Reaction scheme for graft polymerisation and derivatization of the epoxy groups
424 to a DEAE functionality by either cerium ion-initiated or gamma ray-initiated routes.

425 **Figure 2:** SEM photographs of base material (untreated backbone, 2a and 2b), epoxy
426 backbone of monolithic cryogels (2c and 2d), and derivatization of the epoxy groups to a
427 DEAE functionality (2e and 2f).

428 **Figure 3:** Column efficiency versus flow velocity for GIR-DEAE (■) and CG-DEAE (●),
429 using 10 μ L pulse of acetone (5% v/v) and a mobile phase of 20 mM Tris-HCl buffer (pH
430 7.4).

431 **Figure 4:** Determination of Δt ($|\Delta pH| > 0$) from pH profile for GIR-DEAE at a flow rate of
432 300 cm/h by switching between buffer A (500 mM phosphate at pH 7.4) and buffer B (20
433 mM phosphate at pH 7.4).

434 **Figure 5:** a) Dynamic binding capacities (mg/mL - solid lines and mg/g - dotted lines) for
435 GIR-DEAE (■) and CG-DEAE (●) at different flow rates using BSA (2 mg/mL) and a
436 mobile phase of 20 mM Tris-HCl buffer (pH 7.4). b) Corresponding Péclet numbers at
437 different flow rates using 10 μ L pulse of acetone (5% v/v) and a mobile phase of 20 mM
438 Tris-HCl buffer (pH 7.4). All experiments have been repeated at least 3 times to confirm the
439 results and have an error of 5% in measurement.

440

440 **Tables with Captions**

441 **Table 1:** Comparison of DBCs of various anion-exchangers. 2 mg/mL solutions of BSA
 442 were used for DBC measurements, while 10 mg/mL solutions of BSA were used for static
 443 binding experiments (incubation time of 3 h).

Adsorbents	DBC at 10% (300 cm/h)	SBC (mg/mL)	Phosphate Capacity (mmol/L)
GIR-DEAE	26 mg/mL	44 ± 4	119
CG-DEAE	3 mg/mL	8 ± 1	-
8% pAAm Cryogels	1.3 mg/mL ^a	-	-
CIM DEAE	≤ 21 mg/mL ^b	-	1200
WAX poly(GMA-co-PEGDA)	32 mg/mL ^c	-	-
Poly(DEAEMA-co-PEGDA)	24 mg/mL ^c	-	-
PEI poly(GMA-co-EDMA)	14 mg/mL ^d	-	-
Toyopearl DEAE 650 M	20 mg/mL ^e	-	-
MacroPrep DEAE	16 mg/mL ^e	-	-
DEAE Sepharose FF	42 mg/mL	-	113

444 ^aTaken from reference (295 cm/h) [14]. ^bTaken from reference [11]. ^cTaken from reference (203 cm/h) [8].

445 ^dTaken from reference (150 cm/h) [36] ^eTaken from reference (600 cm/h) [37]

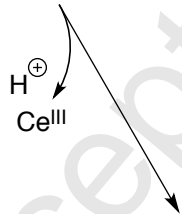
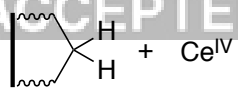
446

- 446 • Highlights
- 447 • Anion-exchange monolithic adsorbents have BSA binding capacity of 110 mg/mL
- 448 • Cryogels are grafted with radiation-induced polymerization of methacrylate
449 monomers.
- 450 • Higher binding capacities for radiation-induced grafting over chemical grafting.
- 451 • Adsorbent pore sizes range from 10 - 100 μm with elastic sponge-like structure.
- 452

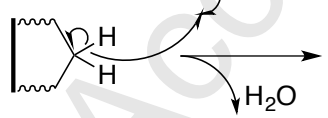
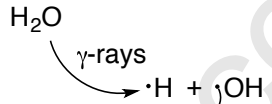
Accepted Manuscript

Figure 1

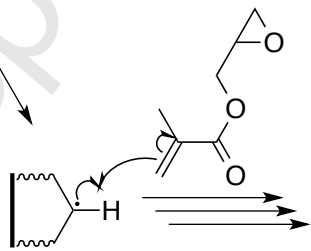
Route 1:
Chemical Grafting



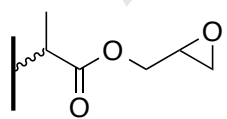
Route 2:
Radiation Grafting



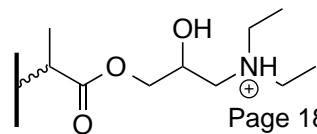
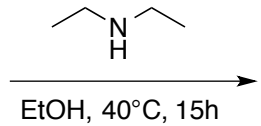
MP-CM



MP-EP



MP-EP



MP-DEAE

Figure 2

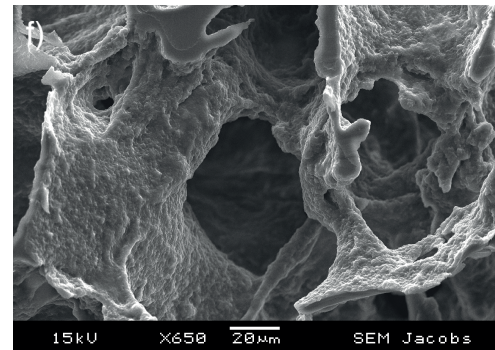
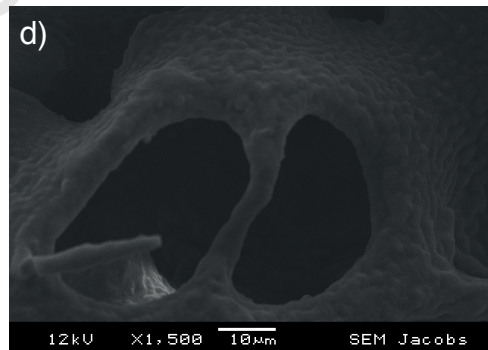
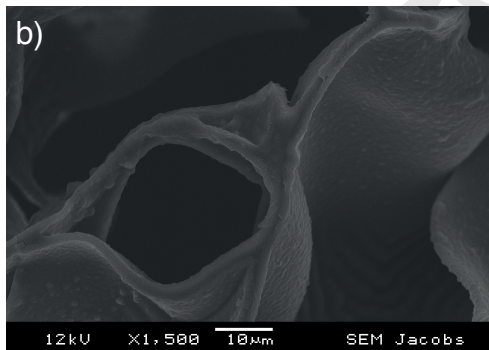
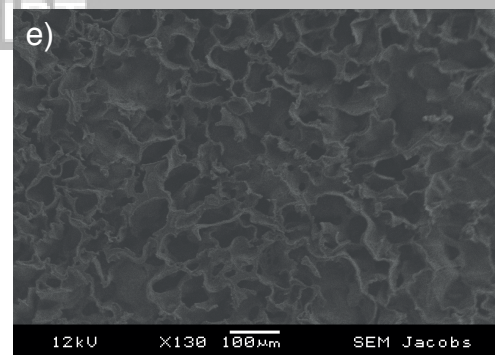
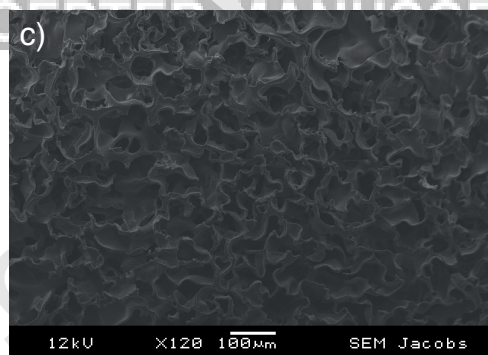
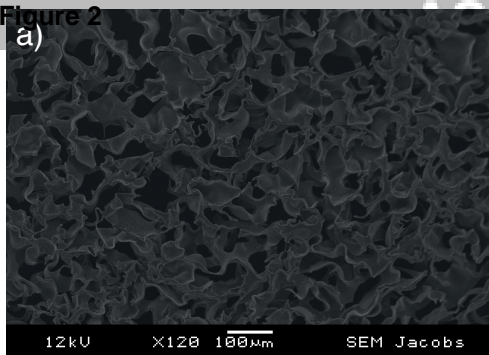
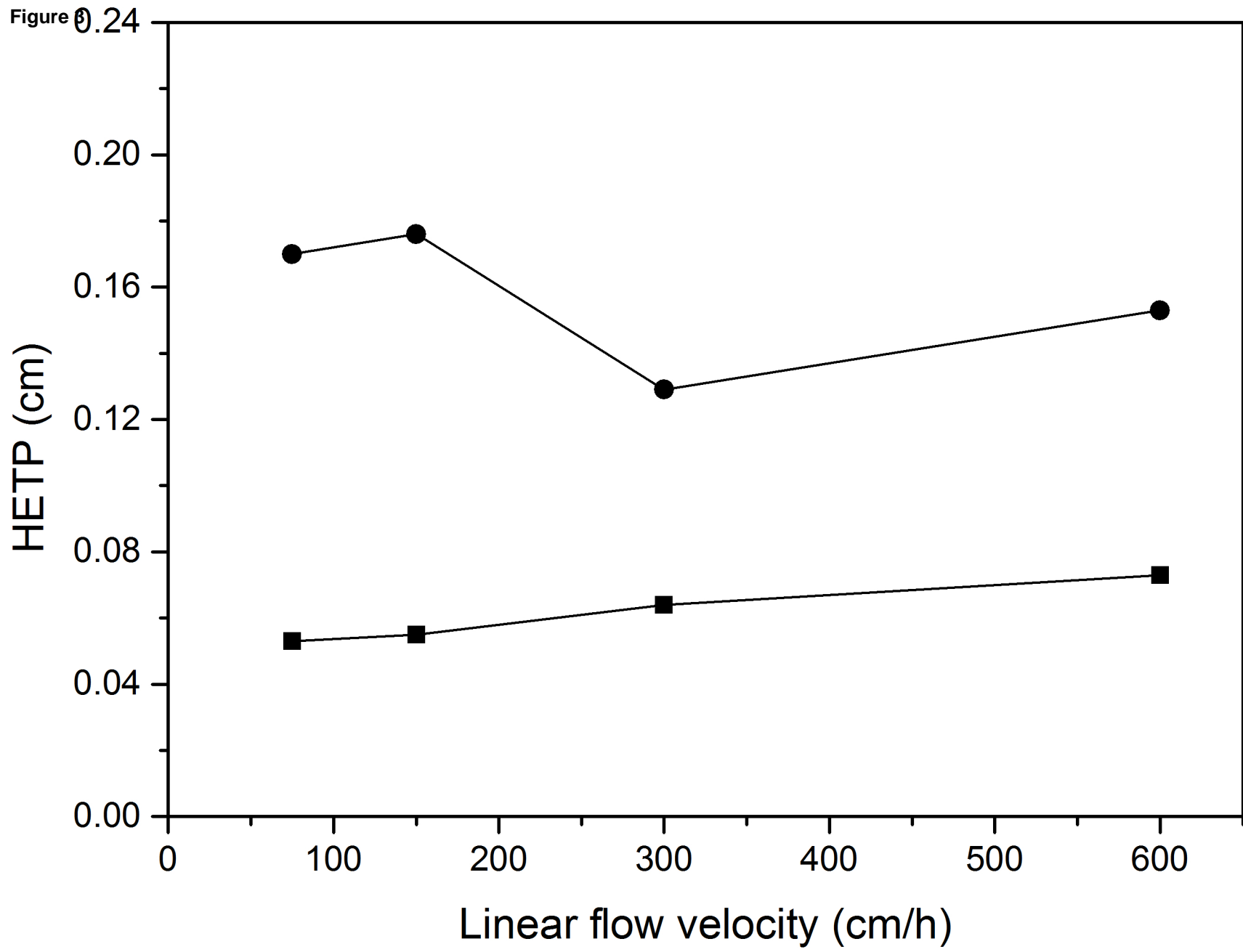
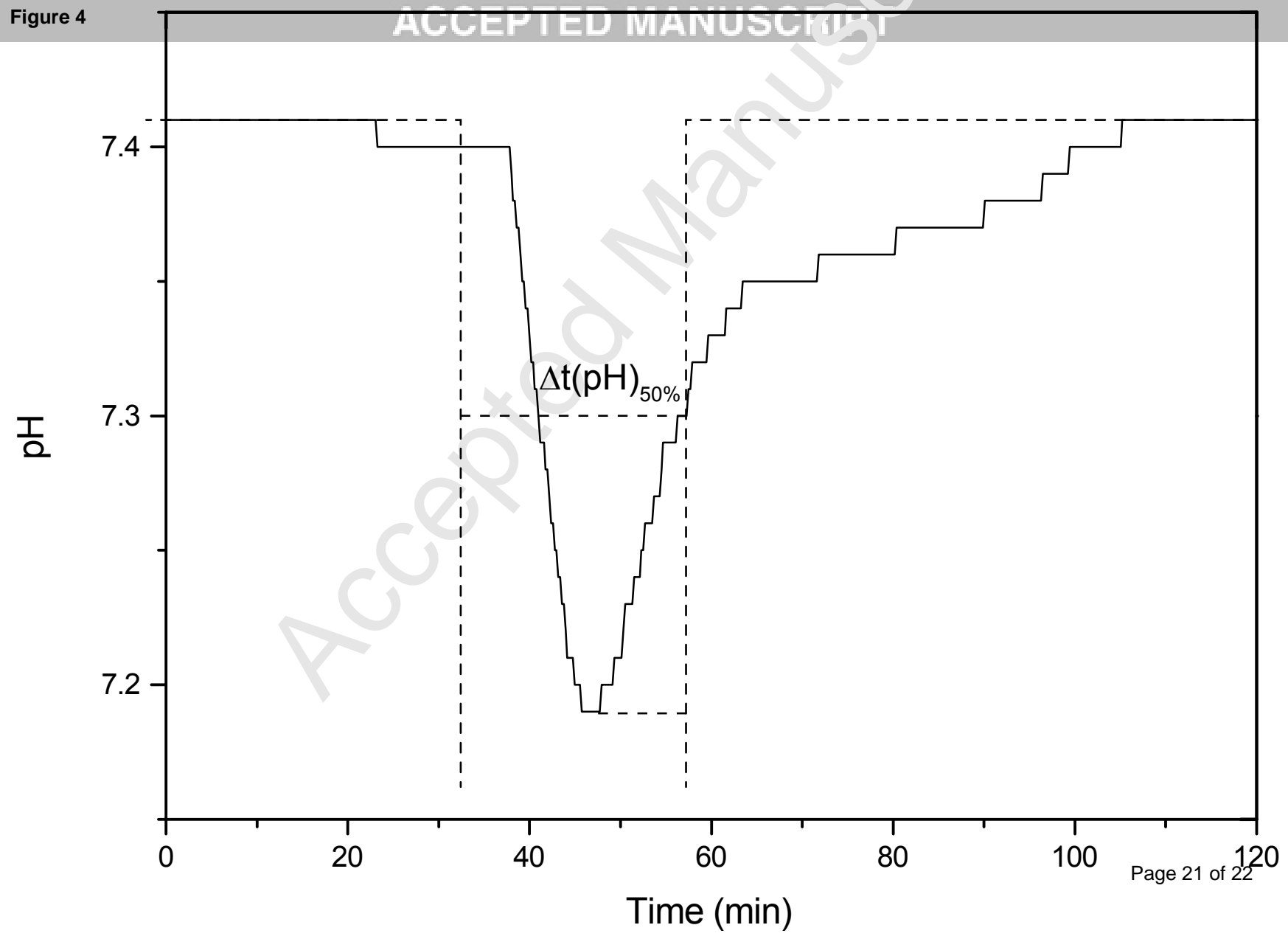
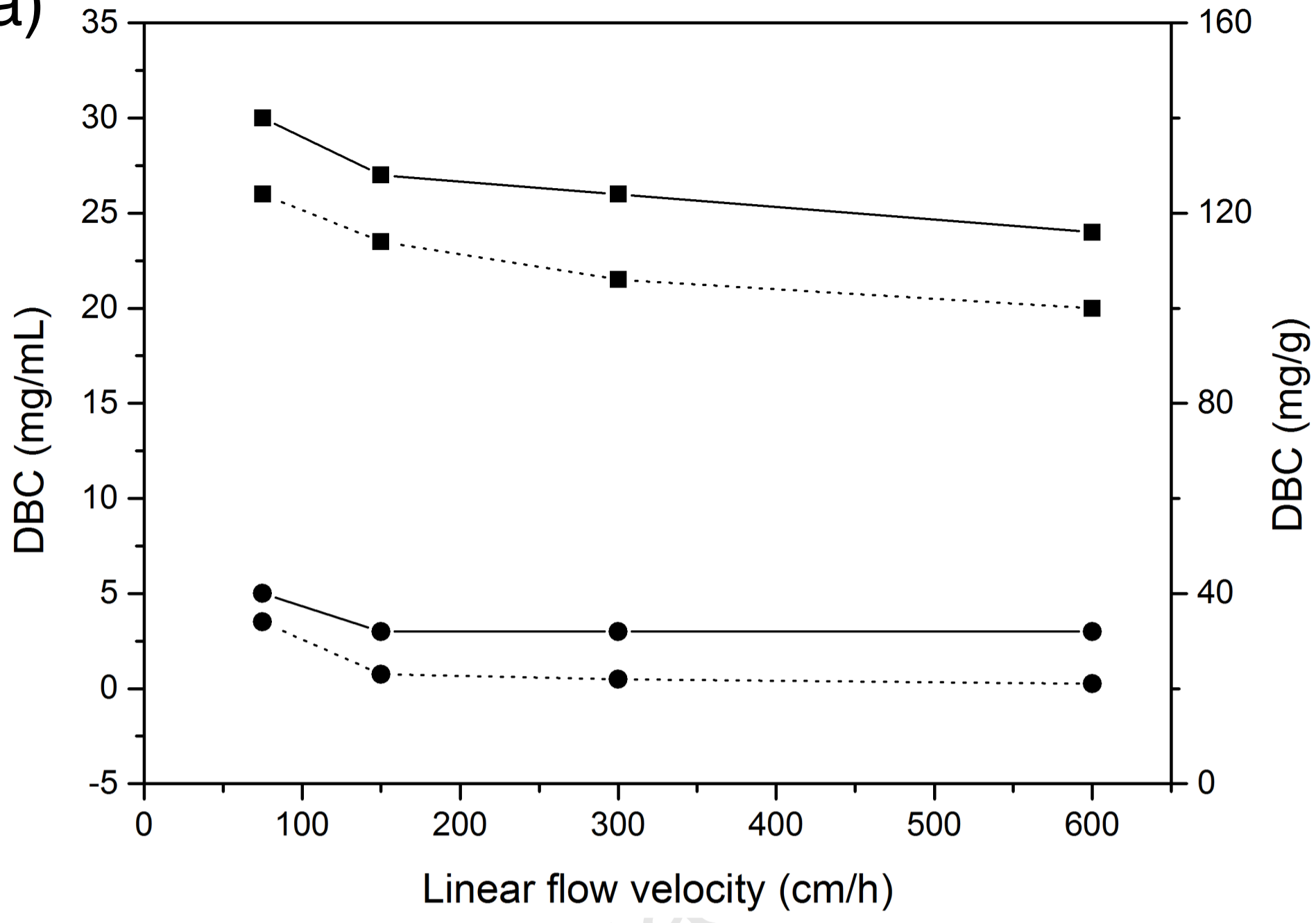


Figure 8





a)



b)

